Quaternary Research 81 (2014) 424–432

Contents lists available at ScienceDirect

Quaternary Research

journal homepage: www.elsevier.com/locate/yqres

Quaternary structural partitioning within the rigid Tarim plate inferred from magnetostratigraphy and sedimentation rate in the eastern Tarim Basin in China

Hong Chang [a], Zhisheng An [a], Weiguo Liu [a], Hong Ao [a], Xiaoke Qiang [a], Yougui Song [a], Zhongping Lai [b]

[a] State Key Laboratory of Loess and Quaternary Geology, Institute of Earth Environment, Chinese Academy of Sciences, Xi'an 710075, China
[b] Resources & Chemical Laboratory, Qinghai Institute of Salt Lakes, Chinese Academy of Sciences, Lanzhou 730000, China

ARTICLE INFO

Article history:
Received 17 March 2013
Available online 7 December 2013

Keywords:
Tarim Basin
Sub-basin structural units
Magnetostratigraphy
Pleistocene
Sedimentation rate
Magnetic susceptibility
Climate change
Tectonic uplift

ABSTRACT

It has been proposed that within the Tarim Basin tectonic activity has been limited since Triassic time. However, on the basis of magnetostratigraphy from the eastern Tarim Basin, which defines the chronology of sedimentation and structural evolution of the basin, we show that the basin interior has been uplifted and partitioned during Quaternary. The magnetostratigraphy was constructed from 2228 samples that yielded acceptable inclination values. Characteristic remnant magnetization (ChRM) with both normal (N1–N11) and reversed (R1–R11) polarity was isolated by thermal demagnetization. The data correlate best with polarity chrons C3r to C1n, which range from 5.39 Ma to recent on the geological time scale 2004 (GTS2004). An abrupt decrease in the sedimentation rate is observed at 1.77 Ma in the Ls1 core. This change does not overlap with known Pleistocene climate-change events. We attribute this sedimentation rate decrease to a structurally controlled local decrease in accommodation space where basin basement uplifts occur. This period of sedimentary environmental change reveals that structural partitioning in the basement of the Tarim Basin occurred since ~1.77 Ma, and we speculate that tilting of the Southeast Uplift (a sub-basin unit) within the Tarim Basin began in early Pleistocene time.

Introduction

The Tarim Basin in northwestern China is widely thought to have behaved rigidly since Triassic time (Jia, 1997). The basin is bounded on the north by the south-verging thrust faults of the southern Tian Shan and on the south by the left-lateral Altyn Tagh strike-slip fault and north-verging thrust faults (Fig. 1). Uplift of the bounding ranges has occurred during Cenozoic time in response to convergence between India and stable Asia (Hendrix et al., 1994; Hao et al., 2002; Wang et al., 2003; Sobel et al., 2006; Negredo et al., 2007). However, the central Tarim Basin has sustained little or no deformation during the India–Asia collision (e.g., Jia, 1993; Yang and Liu, 2002). The relatively rigid behavior of the basin and its structural relationship to the north margin of the Tibetan Plateau, as well as geophysical observations, have led to the suggestion that the lithosphere of the Tarim Basin has subducted southward beneath the northern Tibetan Plateau and northward beneath the Tian Shan since the onset of the India–Asia collision at ~50 Ma (Besse et al., 1984; Garzanti et al., 1987; Searle et al., 1987; Wittlinger et al., 1998; Tapponnier et al., 2001). Seismic images show the depth of Moho discontinuity beneath the Tarim Basin at 42 km depth along its northern margin and at ~57 km beneath the Kunlun foreland (Gao et al., 2000; Kao et al., 2001). Deformation within the upper mantle along the Tarim plate has been observed beneath the Tibetan Plateau (Kao et al., 2001), but few data demonstrate Cenozoic deformation within the basement of the Tarim Basin.

The depositional successions within the basin provide the most tangible and accessible records of the lithological, geographical developments, which occur in a specific area over a specific period of time (Rowley and Currie, 2006; Fang et al., 2007; Wang et al., 2008). In recent years there has been an increase in the number of studies aiming to unravel the links between tectonic events and sedimentary response on a basin scale (Blair and Bilodeau, 1988; Gupta, 1997; Yin et al., 2002; Sun et al., 2008; Lu and Xiong, 2009; Chang et al., 2012a; Xiao et al., 2012). Additionally, tectonic activity also controls the internal basin conformation. The development of smaller intra-basinal faults may influence the internal structure of the basin, partitioning it into related, but separate depocenters (Tankard et al., 1989; Dong et al., 2012). Tectonic activity, therefore, is a fundamental control on sedimentation in basins. The sedimentary sequences within a basin can be related to the tectonic activity that controlled their deposition. The records contained within the basin sediments are important to evaluate the tectono-sedimentary evolution of a region (McCann and Saintot, 2003; Wang et al., 2006). Some aspects of the relationship between tectonic activity and sedimentation can be recognized although the relationship is complex. The nearly 10-km-thick Cenozoic sedimentary rocks derived from the surrounding mountains (Jia, 1997) in the Tarim Basin provide effective constraints on the deformation history of the Tarim Basin. In order to test whether and when (if it was the case) the basement deformation occurred, we examine the sediments in the Tarim Basin because sedimentary process in the basin is sensitive to the environmental and tectonic change (Yin et al., 2008).

0033-5894/$ – see front matter
http://dx.doi.org/10.1016/j.yqres.2013.10.018

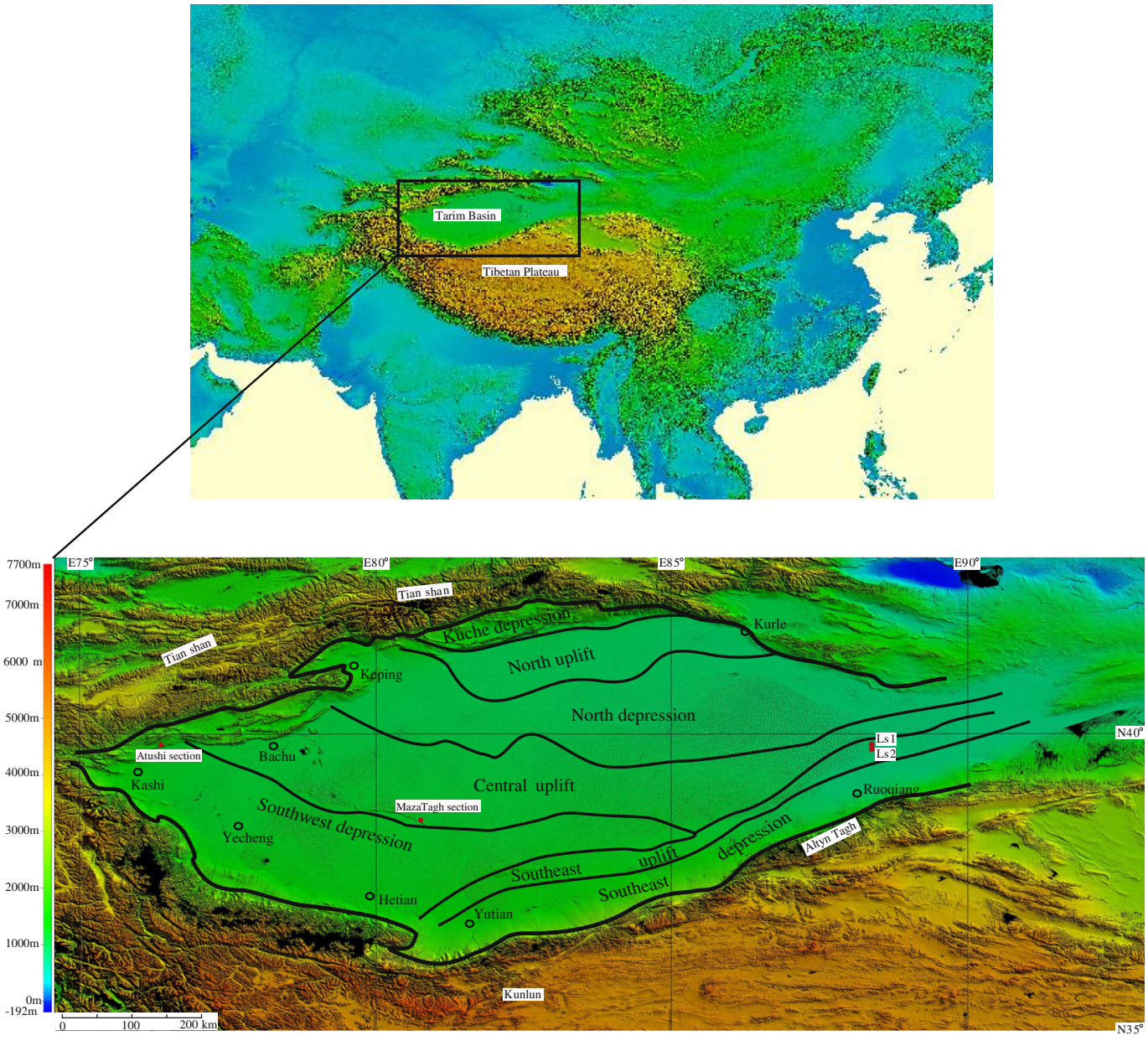

Figure 1. Digital elevation model of the Tarim Basin. The drilling core Ls1, Ls2, natural section, and major geographic locations are located. Boundary of the sub-basin units in the Tarim Basin was portrayed based on Curie isothermic and isopach surfaces of the strata of Cenozoic (Yan and Mu, 1990; Chen et al., 1998; Li and Xu, 1999).

We investigated sedimentation in the southeastern Tarim Basin to understand the tectonic behavior of the Tarim plate and its relationship to the northern Tibet Plateau during late Cenozoic time. We determined magnetostratigraphic ages and sedimentary facies for a drill core (Ls1) from 0.00 to 751.98 m depth. The results show significant changes in sediment accumulation rates over the past ~5.39 Ma, especially at 1.77 Ma. We interpret this variability to reflect deformation patterns controlled by regional tectonics during Pliocene–Quaternary time.

Regional setting

The Tarim Basin has an area of 560,000 km^2 and an elevation of ~1200 m asl. It is typically divided into sub-basin structural units based on Curie isothermic and isopach surfaces of the strata of Cenozoic (i.e., Southwest Depression, Central Uplift, North Depression, North Uplift, Kuche Depression, Southeast Uplift and Southeast Depression) (Yan and Mu, 1990; Chen et al., 1998; Li and Xu, 1999; Fig. 1). The geological structures of the depression include fault lines in and around the depression that have been identified by field geological surveys, magnetic airborne surveys, and remote-sensing images, including aerial photographs and satellite images. These evidences have revealed that the depression is a tectonically active area within well-developed faults and fractures, even though its present surface topography is very flat (GGXCI, 1978; Liang, 1987; Wang, 1987a, 1987b; BGMRXUAR, 1993; Guo and Zhang, 1995; Yan et al., 1998; Zheng et al., 2000; Wang and Liu, 2001; Chen et al., 2002; Huang et al., 2006; Liu et al., 2006; Heermance et al., 2007; Meng et al., 2010; Dong et al., 2012).

The Neoproterozoic basement of the Tarim Basin is overlain by late Precambrian–Cenozoic strata, locally in excess of 15 km thick (Jia, 1993). The northern margin of the Tarim Basin is thought to have collided with the southern Tian Shan in late Devonian time during the amalgamation of Central Asia (Windley et al., 1990; Avouac et al., 1993). The southern margin of the Tarim Basin is thought to have collided with the (Western) Kunlun terrane during Silurian time (Matte et al., 1996).

https://doi.org/10.1016/j.yqres.2013.10.018 Published online by Cambridge University Press

Little deformation in the interior and intense deformation along its margins characterizes the Tarim Basin during Paleozoic time (Jia and Wei, 2002), however, a foreland basin began to develop in Mesozoic time (Matte et al., 1996).

Basin-ward thrusting of the Tian Shan and Kunlun during Cenozoic time caused further subsidence deflection of the foreland depressions where Cenozoic sediments are up to 10 km thick around the basin margins (Yang and Liu, 2002; Huang et al., 2006). The Miocene sediments thickness was mainly centered in the Southwest and Kuche depressions. The thickest sediments are also adjacent to the margins of the basin close to the margin thrust belts (Yan and Mu, 1990; Jia, 1997). Miocene strata elsewhere in the basin are typically 500–1200 m thick and have similar lithofacies in the five inner sub-basin units (Yan and Mu, 1990). This suggests that deformation occurred along the northern and southern margins of the Tarim Basin during Miocene time. The areas influenced by foreland basin flexural subsidence are thought to have extended from Miocene to Pliocene time (Yan and Mu, 1990; Chen et al., 1998). Pliocene strata are the thickest along the northern and southern margins of the basin where they are typically 2000–3500 m thick (Yan and Mu, 1990; Chen et al., 1998; Li and Xu, 1999). The similarity in bedding dips of late Miocene–Pliocene strata in Mazartag area suggests that Cenozoic deformation did not propagate appreciably away from the Kunlun to the basement of the Tarim Basin until after ~2.6 Ma (Sun et al., 2008).

Material and methods

The Ls1 core used in our investigation was sampled from the Luobuzhuang area of the eastern Tarim Basin in 2003 (Fig. 1). It is about 12 km to the north of the Ls2 core, which was drilled in 2004 and for which the magnetostratigraphy was published (Chang et al., 2012b). According to mineral composition, grain size, bedding, color, and structure feature, the Ls1 core is similar to corresponding part of the Ls2, and can be divided into three lithologic units from the bottom to the top (Fig. 5). (I) 751.98–713.50 m, blue-gray to gray siltstone intercalated with brown-red claystone; with laminations to ripples bedding, layered or massive structure; (II) 713.50–35.66 m, gray, brown to red clay-rich siltstone intercalated with red-brown claystone, and blue-gray to gray siltstone with parallel bedding, layered and/or massive structure; and (III) 35.66–0 m, massive gray fine-grained sandstone intercalated sand.

After splitting the core in half lengthwise, 2896 blocks of $2 \times 2 \times 2$ cm were labeled for orientation and removed from the core for discrete magnetic measurements. Blocks were sampled at intervals of 10–40 cm. Variability in the sampling interval was a result of favoring finer-grained horizons to coarser-grained ones.

Low-field magnetic susceptibility was measured with a Bartington MS2 meter at a frequency of 470 Hz. Remanence was measured using a 2G cryogenic superconducting magnetometer (Model 755R) housed in the magnetic shielded space (<150 nT) at the Institute of Earth Environment, Chinese Academy of Sciences. All discrete samples were subjected to stepwise thermal demagnetization using a TD-48 thermal demagnetizer. They were stepwise heated to 690°C with temperature increments of 10–50°C. Demagnetization results were evaluated in orthogonal diagram (Zijderceld, 1967) and the principal-component directions were calculated using a least-squares fitting technique (Kirschvink, 1980).

In order to study rock magnetism, temperature-dependent susceptibility (χ–T) curves and stepwise acquisition of the isothermal remanent magnetisation (IRM) were measured on selected samples. χ–T were measured continuously in an argon atmosphere at a frequency of 976 Hz from room temperature up to 700°C and back to room temperature using a KappaBridge magnetic susceptibility meter (model MFK1-

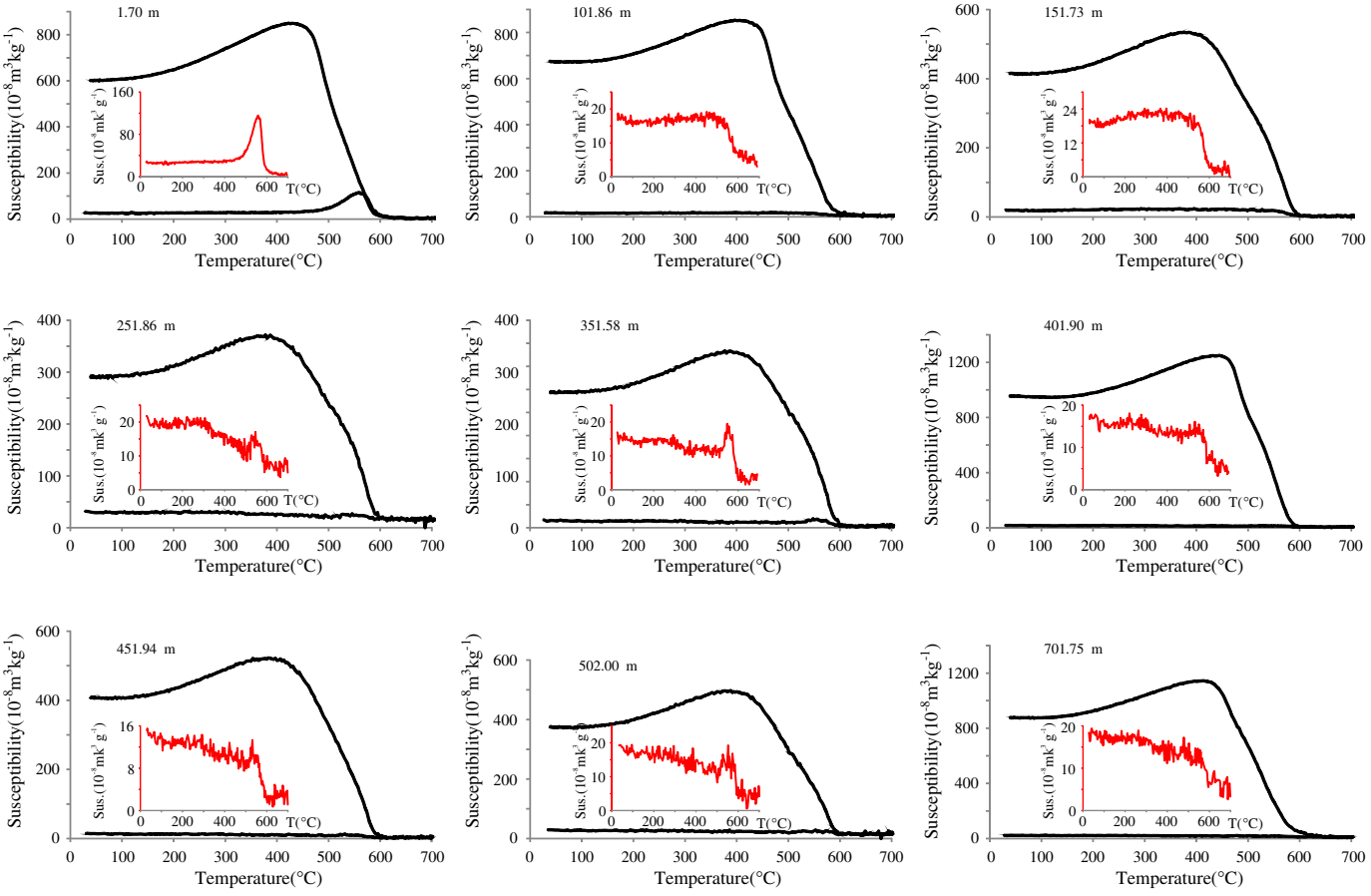

Figure 2. Magnetic susceptibility vs. Temperature (χ–T) curves from selected samples of drill core Ls1. Heating cycles are indicated by the red line in the inset image.

https://doi.org/10.1016/j.yqres.2013.10.018 Published online by Cambridge University Press

FA) equipped with a CS-3 high-temperature furnace (AGICO Ltd., Brno, Czech Republic). IRM acquisitions were determined using an ASC IM-10-30 pulse magnetizer up to saturation IRM (SIRM) at a maximum applied field of 2.7 T and AGICO JR-6A for remanence measurements.

Results

Magnetic mineralogy

Each of the χ–T heating curves undergoes evident decrease near 580°C, which suggests the ubiquitous occurrence of magnetite in the sediments (Fig. 2). χ increases during subsequent cooling after heating to 700°C. This may result from the neoformation of fine-grained magnetite via annealing of iron-containing paramagnetic minerals (Ao et al., 2010). Hematite was not obvious in the χ–T curves due to its weak magnetism, however, all the χ–T curves still displayed a decreased χ between ~580 and ~680°C. Because the bulk susceptibility of magnetite is ~1000× greater than most rock materials (Collinson, 1983), this thermomagnetic behavior suggests that the magnetic minerals are dominated by magnetite and hematite. All the IRM acquisition curves indicate that these samples are not saturated even at 2.7 T (Fig. 3), which is consistent with a significant hematite contribution. Progressive removal of the SIRM by applying reversed fields showed that the remanent coercivities of the SIRM are approximately 45 and 90 mT, indicating that there is high coercive magnetic mineral, such as hematite, that might be predominant within the sediments. These results are in agreement with rock magnetic characteristics from late-Miocene to Holocene sediments in drill core Ls2 in the Tarim Basin (Chang et al., 2012b) and Neogene red beds from the Suerkoli (Xorkoli) basin (Dupont-Nivet and Butler, 2003).

Magnetostratigraphy

For most samples, the high-stability characteristic remnant magnetization (ChRM) component was separated between 400 and 680°C, which suggests that hematite is the dominant remanence carrier (Figs. 4b–h). For some samples, a maximum temperature of 580°C was needed to yield a ChRM component, suggesting that magnetite is the dominant remanence carrier (Fig. 4a). Thermal demagnetization results suggest that magnetite and hematite are the main magnetic minerals in sediments from Ls1 that coincides with research results on rock magnetism using the χ–T curves and IRM methods. More than five successive points in the orthogonal diagrams were used to calculate the direction of ChRM during the establishment of polarity sequence (Fig. 5). Specimens not included in our magnetostratigraphic analysis were rejected based on two criteria. (1) ChRM directions could not be determined because of ambiguous or noisy orthogonal demagnetization diagrams. (2) Effective ChRM directions have maximum angular deviation below 10° and their inclinations are between 15° and 75°. Finally, a total of 2228 (77%) samples gave ChRM directions.

Magnetostratigraphic study result suggests that the Ls1 core recorded 11 normal and 11 reversal magnetozones (Fig. 5). Sediments at the top of the core are Holocene, deposited within the past 100 yr (Zhong et al., 2005). The magnetic polarity sequence yielded from Ls1 was calibrated to the Geological Time Scales (GTS2004) (Gradstein, Ogg and Smith, 2004). Local magnetozone N1 should thus correlate to the chron C1n of GTS2004, consistent with the other researches concerning the age model near Luobuzhuang (Zhong et al., 2005). In the upper part of Ls1, the distinctive reversal polarity with three normal polarities (two are short and one is long) (R1–R4) appears to correlate with GTS2004 from chrons C2r.1r to C1r (Matuyama chron). In the middle part of Ls1, the distinctive magnetozones (N5–N7) are characterized by three normal and two reversals that correlate with the Gauss chron. In the lower part of the Ls1, there are four discrete positive polarities in long reversal polarity (R7–R11). This distinctive and well established magnetozones readily correlate to chrons C3r to C2Ar of the GTS2004. We did not find any obvious hiatuses or scour surfaces in the Ls1 core, and the top sediments are assigned to Holocene time (Zhong et al., 2005). These observations imply that Ls1 core has

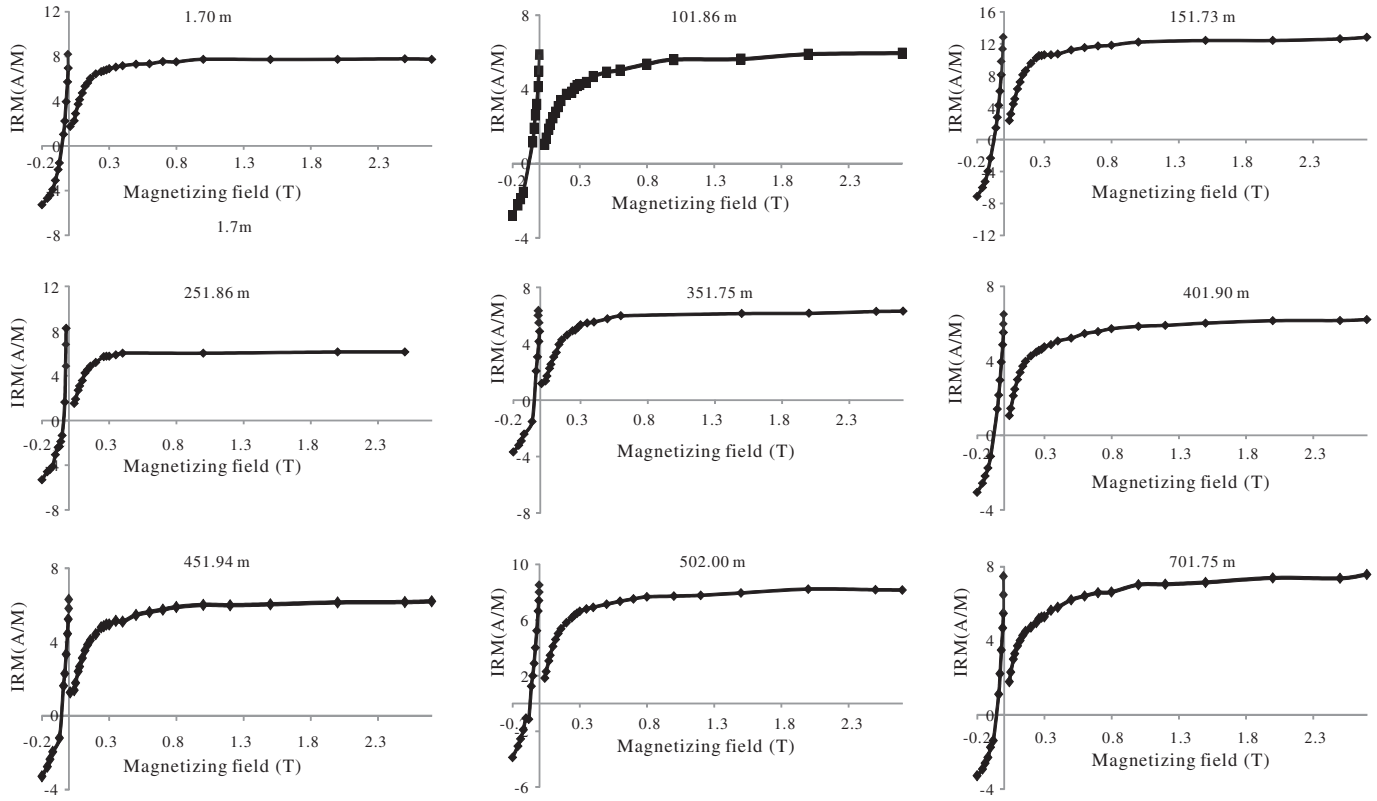

Figure 3. Isothermal remanent magnetization (IRM) acquisition curves for selected samples from the drill core Ls1. Numbers at the top of the graphs represent core depth in meters.

https://doi.org/10.1016/j.yqres.2013.10.018 Published online by Cambridge University Press

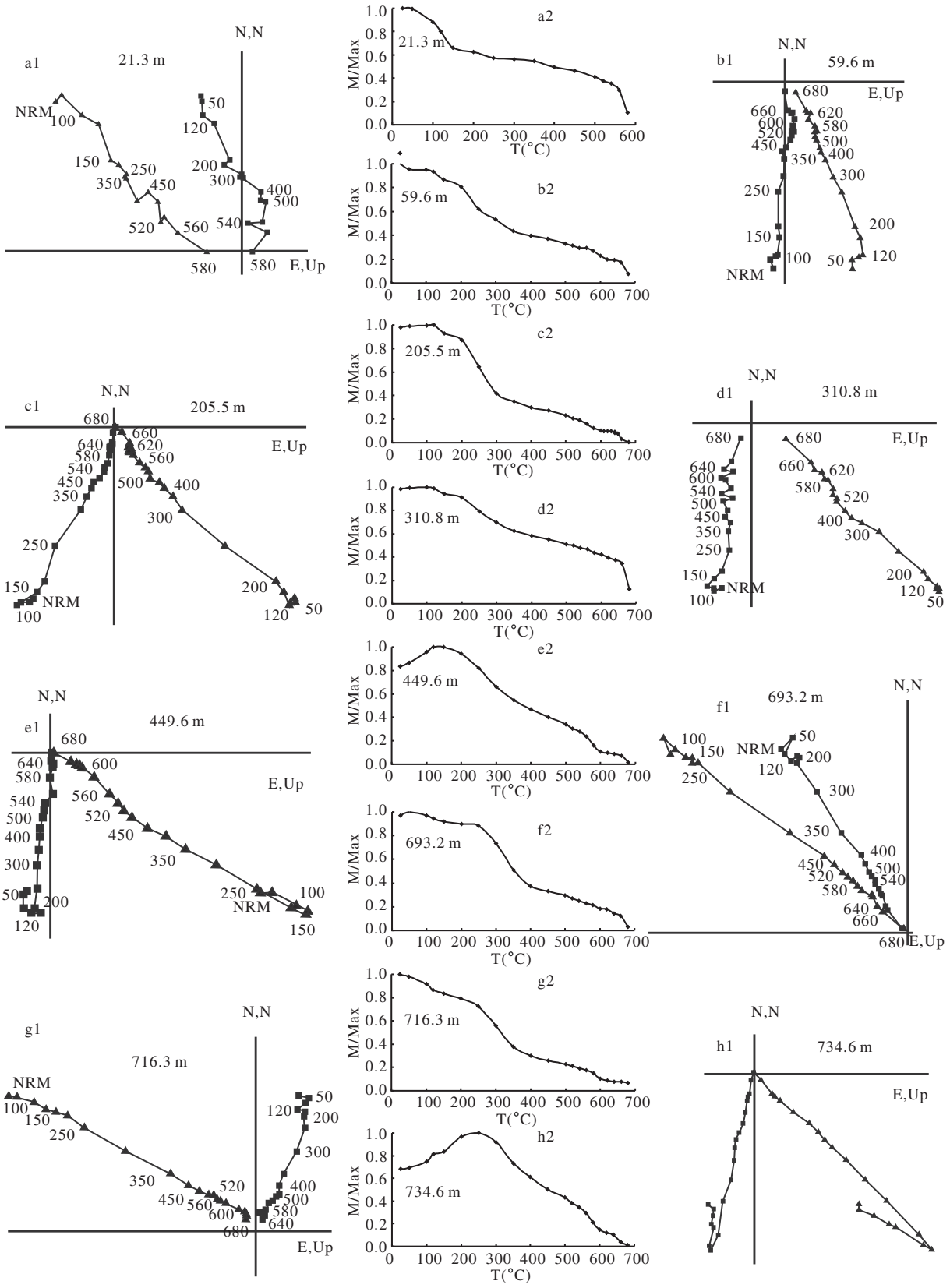

Figure 4. Orthogonal projections of representative progressive thermal demagnetization for selected samples from the drilling core Ls1. The triangles and rectangles represent the vertical and horizontal planes respectively. The numbers refer to the temperatures in °C. NRM is the natural remanent magnetization.

recorded a nearly continuous magnetic polarity sequence from C3r to C1n (~5.39–0.00 Ma). The Pliocene/Pleistocene (~2.58 Ma) and Miocene/Pliocene (~5.33 Ma) boundaries are located at 229.22 m and 742.30 m depth in the Ls1 core, respectively. The Pliocene sedimentary package is 513.08 m thick and is consistent with isopach maps for the southeastern Tarim Basin (Yan and Mu, 1990).

https://doi.org/10.1016/j.yqres.2013.10.018 Published online by Cambridge University Press

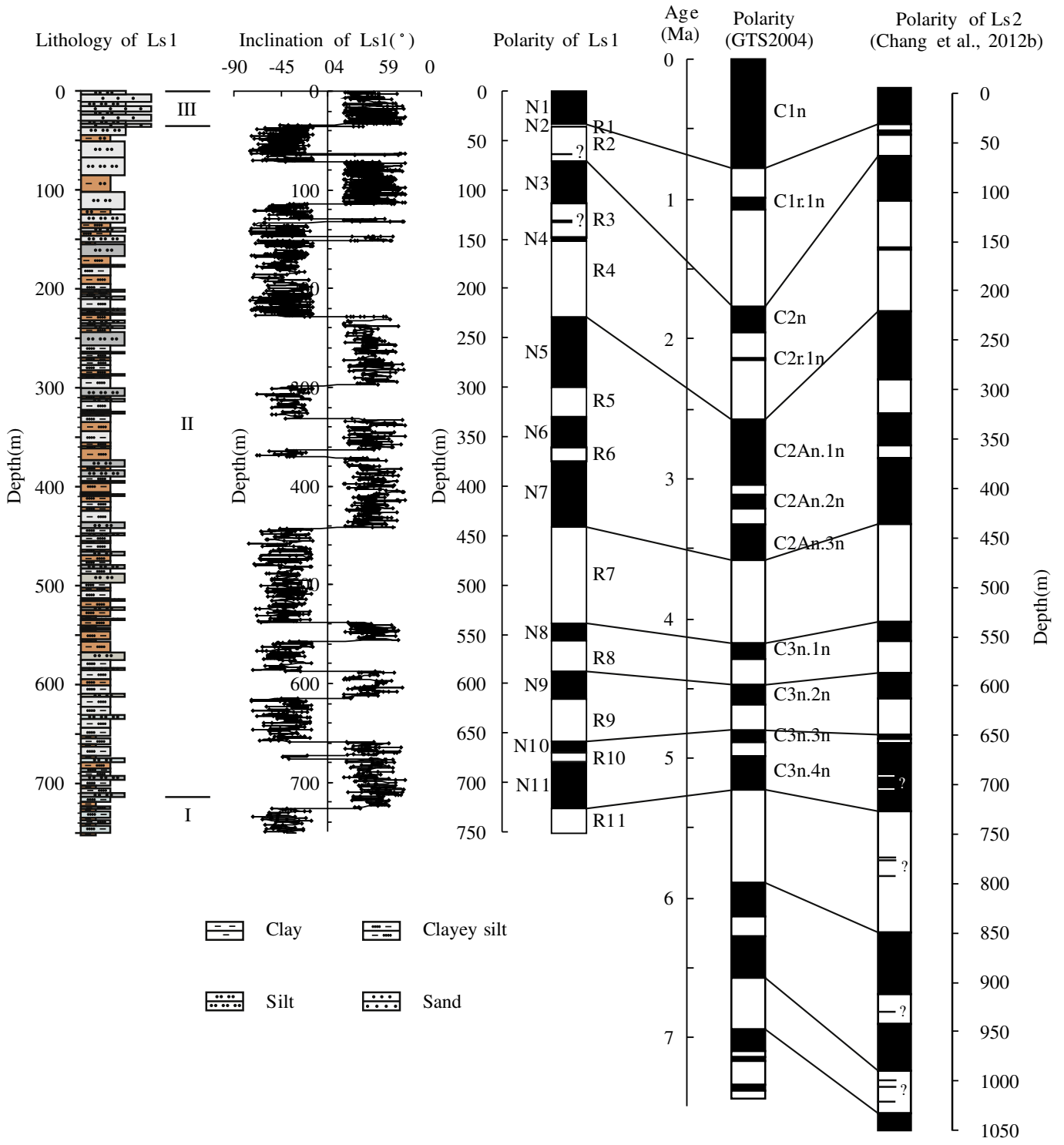

Figure 5. Lithology determined magnetostratigraphy of the Ls1 core in the eastern Tarim Basin, and correlation with geological time scale (Gradstein et al., 2004) and magneto-stratigraphy of the Ls2 (Chang et al., 2012b). The colors in lithology of Ls1 represent the actual color of sediments.

Magnetostratigraphic features of Ls1 are similar to the corresponding depth of Ls2 that is about 12 km to the south (Fig. 5) (Chang et al., 2012b).

Significant changes in the rate of sedimentation were observed in our investigation of the Ls1 core. The average sedimentation rate recorded in the core is ~140 m/Ma. The sediment accumulation rate decreased significantly at ~3.3 Ma, ~3.0 Ma, and ~1.77 Ma (Fig. 6). The sedimentation rate remained steady with only minor fluctuations from 5.39 to 3.58 Ma, 3.04 to 1.77 Ma, and 1.77 to 0.0 Ma.

Discussion

The most obvious change of sedimentation rate occurred at ~1.77 Ma at the depth of 70.98 m, where it decreased from 185 m/Ma to 40 m/Ma (Fig. 6). This sharp sedimentation rate change is also supported by results from Ls2 (Chang et al., 2012b). Sediment-accumulation rates within terrestrial basins are controlled primarily by the sediment supply and accommodation space. Sediment supply is generally a function of climate, stream power (Nott and Roberts,

https://doi.org/10.1016/j.yqres.2013.10.018 Published online by Cambridge University Press

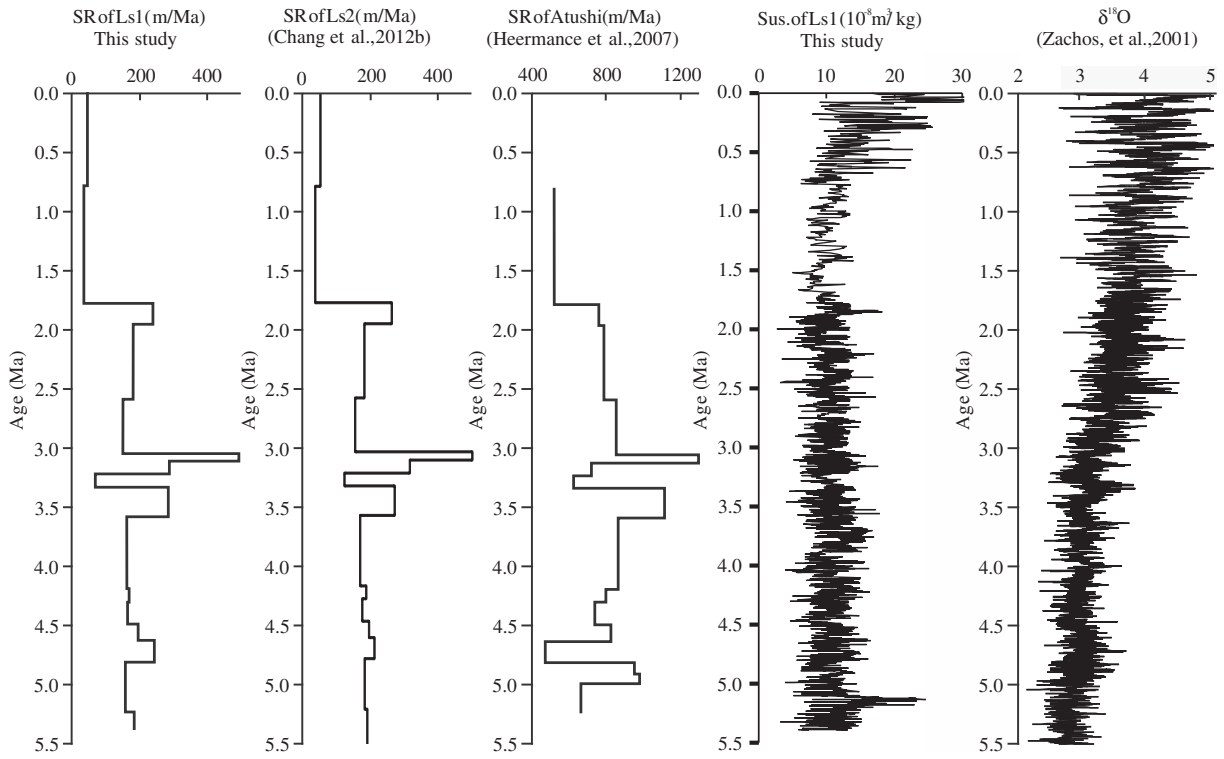

Figure 6. Showing comparing sedimentation rate of the drill core Ls1 to the sedimentation of Ls2, sedimentation rate in Atushi section (Heermance et al., 2007), susceptibility of Ls1 and global deep-sea oxygen isotope curve (Zachos et al., 2001), respectively. SR = sedimentation rate, Sus. = magnetic susceptibility.

1996; Zhang et al., 2001), source-rock lithology or resistance to weathering (Sklar and Dittrich, 2001), and the proximity of the sediment source (Burbank and Beck, 1991). Accommodation space is created when the crust subsides and is caused by: 1) attenuation of the crust due to stretching; 2) contraction of the lithosphere due to cooling; and 3) depression of both crust and lithosphere by sedimentary or tectonic loading. The primary mechanisms of basin subsidence are isostasy, flexure, and cooling effects of lithosphere (Beaumont, 1981).

Sedimentation rate may be influenced by both tectonism and climatic change (Molnar and England, 1990). In the current case, the climatic-control hypothesis can be excluded because of the following two lines of evidence. (1) The frequency and amplitude of global climate variability have increased markedly since 3 Ma (Lisiecki and Raymo, 2007), however this variability is not in phase with sediment-accumulation rates recorded in the Ls1 core. It must be concluded that global climatic change is not the predominant factor that controls the sedimentation rate in the Tarim Basin. (2) The sediments are composed of clay-rich siltstone intercalated with claystone. There are no hiatuses or other evidence that suggest that lithofacies changed during early Pleistocene. Therefore, Ls1 does not show sharp lithofacies changes in the range of 5.0–0.7 Ma.

Furthermore, the climate as revealed by magnetic susceptibility did not obviously change during Pliocene to early Pleistocene (Chang et al., 2012b; Fig. 6). Both the lithology and ostrocods assemblage in the northern Tarim Basin also showed that there was no obvious climatic change during the early Pleistocene (Sun et al., 1999). It follows that local climatic change is not the primary factor that triggered the decrease in sedimentation rate since the early Pleistocene.

On the other hand, there are four clues that call our attention to tectonic influence on the sedimentary environment in the Tarim Basin. (1) Although small in magnitude, earthquakes have occurred inside the Tarim Basin (Xiao et al., 2004). (2) The mantle heat-flow density is generally less than 20 $\mu W/m^2$ in depressions of the Tarim Basin, but it is higher than the value in the higher blocks separating them (Wang et al., 1996). This suggests that mantle heat flow density is imbalance between the elevated blocks and depressions. (3) The Moho is about 40 km deep in the elevated block, but 57 km beneath the Southwest Depression (Gao et al., 2000). Changes in the depth of the Moho suggest that the basement of the Tarim Basin has deformed in the past. (4) The Pliocene–Pleistocene sediments have deformed in the middle of the Tarim Basin (Sun et al., 2008). We propose that the sedimentation rate decrease at ~1.77 Ma indicates onset of shortening and rock uplift that occurred in the elevated sub-basin structural units during Quaternary time. As a corollary, the sedimentation rate should increase in depression sub-basin structural units because of an increase in accommodation space when the nearby region is raised. Further study of drill core from sub-basin depressions may be used to test this hypothesis.

The basement of the Tarim Basin began to change during the early Pleistocene, when the southwestern and southeastern parts of the basin were uplifted as a result of the growth of the Tibetan Plateau (Mu et al., 2001; Dong et al., 2012). The NNE–SSW principal compression stress resulting from collision between Indian and Eurasian plates has exerted significant control on the regional geology during the partitioning of the sub-basin structural units (Guo and Zhang, 1995; Wang and Liu, 2001). This explanation is in accordance with the linear structure map of Chinese land (IMDCAGS, 1981).

Yin et al. (2008) also suggested that currently the Tarim Basin is in its initial stage of disintegration, being consumed by thrusting around its rims and inside its interior and will eventually be incorporated into the Tibetan Plateau and the Altyn Tagh fault will be entirely inside the expanded plateau, like the Kunlun fault today. The depth of the Moho discontinuity beneath the Tarim Basin, 42 km along its northern margin and at ~57 km depth beneath Kunlun foreland (Gao et al., 2000; Kao

https://doi.org/10.1016/j.yqres.2013.10.018 Published online by Cambridge University Press

et al., 2001) suggests that the rigid Tarim Basin has partitioned in the past. The formation of the sub-basin structural units of the Tarim Basin may be the part of this process.

The drill core Ls1 sample is located in the Southeast Uplift of the Tarim Basin (Fig. 1). Shortening and rock uplift of the Southeast Uplift reduced accommodation space, resulting in the decreased sedimentation rate at 1.77 Ma. This structural control in the sedimentation rate is supported by growth strata documented along the Atushi (Fig. 1) from the western Tarim Basin that indicate basement deformation there, likely from 1.9 to 1.4 Ma (Chen et al., 2002; Scharer et al., 2006; Heermance et al., 2007).

We suggest that the Southeast Uplift of the Tarim Basin was structurally uplifted and segmented from the Central Uplift since ~1.77 Ma. This uplift and partitioning would have resulted in a decreased sedimentation rate in the uplifted sub-basin unit.

Conglomeratic facies are often localized near the mountain front where streams flow into the foreland basin and lose much of their sediment-transport capacity. Grain size should naturally decrease into the foreland as a result of the decreasing river gradient within the basin (Scharer et al., 2006). Dispersion of gravel suggests a tectonic coupling that is independent of climatic influences if it can be linked into initiation and growth of specific structures. In order to study specific timing of initiation of individual thrust faults and folds in the Tarim Basin, Heermance et al. (2007) studied 14 sections in the foreland basin in the Southwest Depression in Atushi region of the Tarim Basin. Their data suggest that the basal age of the conglomerate varies from 15.5 ± 0.5 Ma at the northernmost part of the foreland basin in the Southwest Depression, to 8.6 ± 0.1 Ma in the central part of the foreland and to 1.9 ± 0.2 Ma, ~1.04 and 0.7 ± 0.1 Ma along the southern deformation front of the foreland basin. The Atushi section shows a similar rapid sedimentation rate decrease at approximately the same time in the transition zone between the Southwest Depression and the Central Uplift sub-basins (Heermance et al., 2007).

Jin et al (2003) explored Cenozoic deposition sequences in the piedmont along the west Kunlun and discovered that molasse deposition was interrupted in the early Pleistocene by a tectonic pulse, which resulted in tilting of the molasse and underlying sediments at high-angle towards the Tarim Basin. Recent research on high-resolution magnetostratigraphy and sedimentation shows that both the strongest tectonic deformation and changes from deposition to erosion since 1.8 Ma (Fang et al., 2007).

Studies of the geomorphology and stratigraphy in the northeastern Tibetan Plateau suggest that there has been strong uplift of the northeast plateau since 1.7 Ma, and this is when the Yellow river drainage system started to form in the Longzhong Basin (Li et al., 1996, 1997). The independent evidences of tectonic movement in the northeast part of the Tibetan Plateau and the Tarim Basin support the inference that the Tarim Basin will eventually be incorporated into the Tibetan Plateau and the Altyn Tagh fault will be entirely inside the expanded plateau in the future (Yin et al., 2008).

Conclusions

It has been proposed that the Tarim Basin has behaved rigidly since Triassic time, and that the tectonic activity is limited inside the basin. However, the current study shows that the interior of the basin has uplifted and partitioned during Quaternary time.

Our magnetostratigraphy investigation of drill core Ls1 provides the detailed age control for the upper Cenozoic strata from the inner Tarim Basin. The base of the Ls1 core is ~5.39 Ma, whereas the top is Holocene in age. The sedimentation rate in the eastern Tarim Basin decreased rapidly at 1.77 Ma from about ~185 m/Ma to 40 m/Ma. This decrease resulted primarily from the basement involved shortening and rock uplift and occurred contemporaneous with shortening in the northwestern Tarim Basin (Heermance et al., 2007). The Southeast Uplift and Depression sub-basins began to separate tectonically by ~1.77 Ma. The tectonic deformation in the northeastern Tibetan Plateau represents a possible future structural development for crust now present in the Tarim Basin.

Acknowledgments

This research was conjunctly supported by NSFC (40921120406, 41290252) and the Tibetan Plateau Special Project from the Chinese Academy of Sciences (XDB03020102), and National Basic Research Program of China (2010CB833400). We thank Peter Molnar, Morin Clark and Alexander Pullen for their comments and for improving the English.

References

Ao, H., Deng, C.L., Dekkers, M.J., Liu, Q.S., 2010. Magnetic mineral dissolution in the Pleistocene fluvial-lacustrine sediments, Nihewan Basin (North China). Earth and Planetary Science Letters 292, 191–200.
Avouac, J.P., Tapponnier, P., Bai, M., Hou, Y., Wang, G., 1993. Active thrusting and folding along the northeastern Tienshan, and rotation of Tarim relative to Dzungaria and Kazakhstan. Journal of Geophysical Research 98, 6755–6804.
Beaumont, C., 1981. Foreland basins. Geophysical Journal of the Royal Astronomical Society 65, 291–329.
Besse, J., Courtillot, V., Pozzi, J.P., Westphal, M., Zhou, Y.X., 1984. Paleomagnetic estimates of crustal shortening in the Himalayan thrusts and Zanbo suture. Nature 311, 621–626.
Blair, T.C., Bilodeau, W.L., 1988. Development of tectonic cyclothems in rift, pull-apart, and foreland basins: sedimentary response to episodic tectonism. Geology 16, 517–520.
Burbank, D.W., Beck, R.A., 1991. Model of aggradation versus progradation in the Himalayan Foreland. Geologische Rundschau 80, 623–638.
Bureau of Geology and Mineral Resources of Xinjiang Uygur Autonomous Region, 1993. Regional Geology of Xinjiang Uygur Autonomous Region. BGMRXYAR Geological Publication House, Beijing.
Chang, H., Ao, H., An, Z.S., Fang, X.M., Song, Y.G., Qiang, X.K., 2012a. Magnetostratigraphy of the Suerkuli Basin indicates Pliocene (3.2 Ma) activity of the middle Altyn Tagh Fault, northern Tibetan Plateau. Journal of Asian Earth Sciences 44, 169–175.
Chang, H., An, Z.S., Liu, W.G., Qiang, X.K., Song, Y.G., Ao, H., 2012b. Magnetostratigraphic and paleoenvironmental records for a Late Cenozoic sedimentary sequence drilled from Lop Nor in the eastern Tarim Basin. Global and Planetary Changes 80–81, 113–122.
Chen, C.M., Lu, H.F., Jia, D., Xie, X.A., 1998. Tertiary–Quaternary sedimentation, tectonic deformation in Tarim basin and its implications to petroleum geology. Acta Sedimentologica Sinica 16, 113–116 (in Chinese with abstract in English).
Chen, J., Burbank, D.W., Scharer, K.M., Sobel, E., Yin, J.H., Rubin, C., Zhao, R.B., 2002. Magnetochronology of the upper Cenozoic strata in the southwestern Chinese Tian Shan: rates of Pleistocene folding and thrusting. Earth and Planetary Science Letters 195, 113–130.
Collinson, D.W., 1983. Methods in Rock Magnetism and Palaeomagnetism: Techniques and Instruments. Chapman & Hall, London.
Dong, Z.B., Lv, P., Qian, G.Q., Xia, X.C., Zhao, Y.J., Mu, G.J., 2012. Research progress in China's Lop Nur. Earth-Science Reviews 111, 142–153.
Dupont-Nivet, G., Butler, R.F., 2003. Paleomagnetism indicates no Neogene vertical axis rotations of the northeastern Tibetan Plateau. Journal of Geophysical Research 108, 2386.
Fang, X.M., Zhang, W.L., Meng, Q.Q., Gao, J.P., Wang, X.M., King, J., Song, C.H., Dai, S., Miao, Y.F., 2007. High-resolution magnetostratigraphy of the Neogene Huaitoutala section in the eastern Qaidam Basin on the NE Tibetan Plateau, Qinghai Province, China and its implication on the tectonic uplift of the NE Tibetan Plateau. Earth and Planetary Science Letters 258, 293–306.
Gao, R., Huang, D.D., Li, D.Y., Qian, G.H., Li, Y.K., Kuang, C.Y., Li, Q.S., Li, P.W., Feng, R.J., Guan, Y., 2000. Deep seismic reflection profile across the juncture zone between the Tarim Basin and the West Kunlun Mountains. Chinese Science Bulletin 45, 2281–2286.
Garzanti, E., Baud, A., Mascale, G., 1987. Sedimentary record of the northward flight on India and its collision with Eurasia (Ladakh, Himalay, India). Geodinamica Acta 1, 297–312.
Geomorphology Group of Xinjiang Comprehensive Investigation (GGXCI), 1978. Geomorphology of Xinjiang. Science Press, Beijing (In Chinese).
Gradstein, F., Ogg, J., Smith, A., 2004. A Geologic Time Scale 2004. Cambridge University Press, Cambridge.
Guo, Z.J., Zhang, Z.C., 1995. The Geological interpretation of the forming and evolution of Lop Nur, NW China. Geological Journal of University 1, 82–87 (In Chinese with English abstract).
Gupta, S., 1997. Tectonic control on paleovalley incision at the distal margin of the early Tertiary Alpine Foreland Basin, southeast France. Journal of Sedimentary Research 67, 1030–1043.
Hao, Y.C., Guan, S.Z., Ye, L.S., Huang, Y.Y., Zhou, Y.C., Guan, S.Q., 2002. Neogene stratigraphy and paleogeography in the western Tarim basin. Acta Geologica Sinica 76, 289–298 (in Chinese with abstract in English).
Heermance, R.V., Chen, J., Burbank, D.W., Wang, C.S., 2007. Chronology and tectonic controls of Late Tertiary deposition in the southwestern Tian Shan foreland, NW China. Basin Research 19, 599–632.

https://doi.org/10.1016/j.yqres.2013.10.018 Published online by Cambridge University Press

Hendrix, M.S., Dumitru, T.A., Graham, S.A., 1994. Late-Oligocene–Early-Miocene unroofing in the Chinese Tien Shan: an early effect of the India–Asia collision. Geology 22, 487–490.
Huang, B.C., Piper, J.D.A., Peng, S.T., Liu, T., Li, Z., Wang, Q.C., Zhu, R.X., 2006. Magnetostratigraphic study of the Kuche Depression, Tarim Basin, and Cenozoic uplift of the Tian Shan Range, Western China. Earth and Planetary Science Letters 251, 346–364.
Institute of Mineral Deposits, Chinese Academy of Geological Sciences (IMDCAGS), 1981. Linear Structure Map of Chinese Lands (1:6000000) (In Chinese). Sinomap Press, Beijing.
Jia, C.Z., 1993. Structural feature and law of hydrocarbon accumulation in the Tarim basin. Xinjiang Petroleum Geology 20, 177–183 (in Chinese with abstract in English).
Jia, C.Z., 1997. Tectonic Characteristics of Tarim Basin in China (in Chinese). Petroleum Industry Publishing House, Beijing.
Jia, C.Z., Wei, G.Q., 2002. Structural characteristics and petroliferous features of Tarim Basin. Chinese Science Bulletin 47 Suppl., 1–11.
Jin, X.C., Wang, J., Chen, B.W., Ren, L.D., 2003. Cenozoic depositional sequences in the piedmont of the west Kunlun and their paleogeographic and tectonic implications. Journal of Asian Earth Sciences 21, 755–765.
Kao, H., Gao, R., Rau, R., Shi, D.N., Chen, R.Y., Guan, Y., Wu, F.T., 2001. Seismic image of the Tarim basin and its collision with Tibet. Geology 29, 575–578.
Kirschvink, J.L., 1980. The least squares line and plane and analysis of paleomagnetic data. Geophysical Journal of the Royal Astronomical Society 62, 699–712.
Li, Q.C., Xu, B.R., 1999. The characteristic and geological meaning of Curie isothermic surface under the Tarim basin. Oil Geology Prospect 34, 590–594 (in Chinese with abstract in English).
Li, J.J., Fang, X.M., Ma, H.Z., Zhu, J.J., Pan, B.T., Chen, H.L., 1996. Geomorphological and environmental evolution in the upper reaches of the Yellow River during the late Cenozoic. Science in China 39, 380–389.
Li, J.J., Fang, X.M., Van der Voo, R., Zhu, J.J., Niocaill, C.M., Cao, J.X., Zhong, W., Chen, H.L., Wang, J.L., Wang, J.M., Zhang, Y.C., 1997. Late Cenozoic magnetostratigraphy (11–0 Ma) of the Dongshanding and Wangjiashan sections in the Longzhong Basin, western China. Geologie en Mijnbouw 76, 121–134.
Liang, K., 1987. The environmental evolution of Lake Lop Nor as seen on the remote sensing images. Remote Sensing of Environment China 2 (4), 285–295 (In Chinese with abstract in English).
Lisiecki, L.E., Raymo, M.E., 2007. Plio-Pleistocene climate evolution: trends and transitions in glacial cycle dynamics. Quaternary Science Reviews 26, 56–69.
Liu, C.L., Wang, M.L., Jiao, P.C., Li, S.D., Chen, Y.Z., 2006. Features and formation mechanism of faults and potash-forming effect in the Lop Nur Salk Lake, Xinjiang, China. Acta Geologica Sinica 80, 936–943.
Lu, H.J., Xiong, S.F., 2009. Magnetostratigraphy of the Dahonggou section, northern Qaidam Basin and its bearing on Cenozoic tectonic evolution of the Qilian Shan and Altyn Tagh Fault. Earth and Planetary Science Letters 288, 539–550.
Matte, P., Tapponnier, P., Arnaud, N., Bourjot, L., Avouac, J.P., Vidal, P., Liu, Q., Pan, Y.S., Wang, Y., 1996. Tectonics of western Tibet, between the Tarim and the Indus. Earth and Planetary Science Letters 142, 311–330.
McCann, T., Saintot, A., 2003. Tracing tectonic deformation using the sedimentary record: an overview. In: McCann, T., Saintot, A. (Eds.), Tracing Tectonic Deformation Using the Sedimentary Record, pp. 1–28.
Meng, G.X., Yan, J.Y., Lv, Q.T., Jiao, P.C., Yan, H., Liu, C.F., Liu, C.L., 2010. New discovery of Lop Nur salt basin structure and its significance for potash deposit exploration. Mineral Deposits 29, 609–615.
Molnar, P., England, P., 1990. Late Cenozoic uplift of mountain ranges and global climate change: chicken or egg? Nature 346, 29–34.
Mu, G.J., Bao, A.M., Hao, J., 2001. Geotectonic environment of the tail-end-lakes evolution, Xinjiang, China. Arid Land Geography 24, 193–200 (in Chinese with abstract in English).
Negredo, A.M., Replumaz, A., Villaseñor, A., Guillot, S., 2007. Modeling the evolution of continental subduction processes in the Pamir–Hindu Kush region. Earth and Planetary Science Letters 259, 212–225.
Nott, J., Roberts, R.G., 1996. Time and process rates over the past 100 m.y.: a case for dramatically increased landscape denudation rates during the late Quaternary in northern Australia. Geology 24, 883–887.
Rowley, D.B., Currie, B.S., 2006. Paleo-altimetry of the late Eocene to Miocene Lunpola basin, central Tibet. Nature 439, 677–681.
Scharer, K.M., Burbank, D.W., Chen, J., Weldon II, R.J., 2006. Konematic models of fluvial terraces over active detachment fold: constraints on the growth mechanism of the Kashi–Atushi fold system, Chinese Tian Shan. Geological Society of America Bulletin 118, 1006–1028.
Searle, M.P., Windley, B.F., Coward, M.P., Cooper, D.J.W., Rex, A.J., Rex, D., Li, T.D., Xiao, X.C., Jan, M.Q., Thakur, V.C., Kumar, S., 1987. The closing of Tethys and the tectonics of the Himalaya. Geological Society of America Bulletin 98, 678–701.
Sklar, L.S., Dittrich, W.E., 2001. Sediment and rock strength controls on river incision into bedrock. Geology 29, 1087–1090.
Sobel, E.R., Chen, J., Heermance, R.V., 2006. Late Oligocene–Early Miocene initiation of shortening in the Southwestern Chinese Tian Shan: implications for Neogene shortening rate variations. Earth and Planetary Science Letters 247, 70–81.
Sun, Z.C., Feng, X.J., Li, D.M., Yang, F., Qu, Y.H., Wang, H.J., 1999. Cenozoic Ostracoda and palaeoenvironments of the northeastern Tarim Basin, western China. Palaeogeography Palaeoclimatology Palaeoecology 148, 37–50.
Sun, J.M., Zhang, L.Y., Deng, C.L., Zhu, R.X., 2008. Evidence for enhanced aridity in the Tarim Basin of China since 5.3 Ma. Quaternary Science Reviews 27, 1012–1023.
Tankard, A.J., Welsink, H.J., Jenkins, W.A.W., 1989. Structural styles and stratigraphy of the Jeanne d'Arc Basin, Grand Banks of Newfoundland. In: Tankard, A.J., Balkwill, H.R. (Eds.), Extensional Tectonics and Stratigraphy of North Atlantic Margins. AAPG Memoir, 46, pp. 265–282.
Tapponnier, P., Xu, Z.Q., Roger, F., Meyer, B., Arnaud, N., Wittlinger, G., Yang, J.S., 2001. Oblique stepwise rise and growth of the Tibetan Plateau. Science 294, 1671–1677.
Wang, S., 1987a. A preliminary study on neotectonic movement in the Lop Nur and surrounding regions. In: Xia, X. (Ed.), Scientific Exploration and Study of the Lop Nor. Science Press, Beijing, pp. 37–51.
Wang, W., 1987b. The geological history of the Lop Nor and surrounding regions. In: Xia, X. (Ed.), Scientific Exploration and Study of the Lop Nor. Science Press, Beijing, pp. 16–19.
Wang, M., Liu, C., 2001. Saline Lake Potash Resources in the Lop Nur. Geological Publishing House, Beijing.
Wang, L.S., Li, C., Yang, C., 1996. The lithospheric thermal structure beneath Tarim Basin, western China. Acta Geophysica Sinica 39 (6), 794–803 (in Chinese with abstract in English).
Wang, E., Van, J.L., Liu, J.Q., 2003. Late Cenozoic geological evolution of the foreland basin bordering the West Kunlun range in Pulu area: constraints on timing of uplift of northern margin of the Tibetan Plateau. Journal of Geophysical Research 108, 2401. http://dx.doi.org/10.1029/2002JB001877.
Wang, E., Xu, F.Y., Zhou, J.X., Wan, J.L., Burchfield, B.C., 2006. Eastward migration of the Qaidam basin and its implications for Cenozoic evolution of the Altyn Tagh fault and associated river system. Geological Society of America Bulletin 118, 349–365.
Wang, C.S., Zhao, X.X., Liu, Z.F., Lippert, P., Graham, S.A., Coe, R.S., Yi, H.S., Zhu, L.D., Liu, S., Li, Y.L., 2008. Constraints on the early uplift history of the Tibetan Plateau. Proceedings of the National Academy of Sciences of the United States of America 105, 4987–4992.
Windley, B.F., Allen, M.B., Zhang, C., Zhao, Z.Y., Wang, G.R., 1990. Paleozoic accretion and Cenozoic redeformation of the Chinese Tien Shan Ranges, central Asia. Geology 18, 128–131.
Wittlinger, G., Tapponnier, P., Poupinet, G., Jiang, M., Shi, D.N., Herquel, G., Masson, F., 1998. Topographic evidence for localized lithospheric shear along the Altyn Tagh Fault. Science 28, 74–76.
Xiao, X.C., Liu, X., Gao, R., et al., 2004. The crustal structure and tectonic evolution of southern Xinjiang China. The Commercial Press, Beijing 1–270.
Xiao, G.Q., Guo, Z.T., Dupont-Nivet, G., Lu, H.Y., Wu, N.Q., Ge, J.Y., Hao, Q.Z., Peng, S.Z., Li, F.J., Abels, H.A., Zhang, K.X., 2012. Evidence for northeastern Tibetan Plateau uplift between 25 and 20 Ma in the sedimentary archive of the Xining Basin, Northwestern China. Earth and Planetary Science Letters 317–318, 185–195.
Yan, S., Mu, G.J., 1990. The environmental evolution of the Tarim Basin in late Cenozoic era. Arid Land Geography 13, 1–9 (in Chinese with abstract in English).
Yan, S., Mu, G.J., Xu, Y.Q., Zhao, Z.H., 1998. Quaternary environmental evolution of the Lop Nur region, China. Acta Geographica Sinica 53, 332–340 (in Chinese with abstract in English).
Yang, Y.Q., Liu, M., 2002. Cenozoic deformation of the Tarim plate and the implications for mountain building in the Tibetan Plateau and the Tian Shan. Tectonics 21, 1059. http://dx.doi.org/10.1029/2001TC001300.
Yin, A., Rumelhart, P.E., Butler, R., Cowgill, E., Harrison, T.M., Foster, D.A., Ingersoll, R.V., Zhang, Q., Zhou, X.Q., Wang, X.F., Hanson, A., Raza, A., 2002. Tectonic history of the Altyn Tagh fault system in northern Tibetan. Geological Society of America Bulletin 114, 1257–1295.
Yin, A., Dang, Y.Q., Zhang, M., Chen, X.H., McRivette, M.W., 2008. Cenozoic tectonic evolution of the Qaidam basin and its surrounding regions (Part 3): structural geology, sedimentation, and regional tectonic reconstruction. Geological Society of America Bulletin 120, 847–876.
Zachos, J., Pagani, M., Sloan, L., Thomas, E., Billups, K., 2001. Trends, rhythms, and aberrations in global climate 65 Ma to present. Science 292, 686–693.
Zhang, P.Z., Molnar, P., Downs, W.R., 2001. Increased sedimentation rates and grain sizes 2–4 Myr ago due to the influence of climate change on erosion rates. Nature 410, 891–897.
Zheng, H.B., Powell, C.M., An, Z.S., Zhou, J., Dong, G.R., 2000. Pliocene uplift of the northern Tibetan Plateau. Geology 28, 715–718.
Zhong, W., Tuerxun, Keyimu, Shu, Q., Wang, L.G., 2005. Paleoclimatic and paleoenvironmental evolution since about 25 Ka BP in the Taitema Lake area, South Xinjiang. Arid Land Geography 28, 183–187 (in Chinese with abstract in English).
Zijderceld, J.D.A., 1967. A.C. demagnetization of rock: analysis of results. In: Collinson, D.W., Creer, K.M., Runcorn, S.K. (Eds.), Methods in Paleomagnetism. Elsevier, New York, pp. 254–286.

https://doi.org/10.1016/j.yqres.2013.10.018 Published online by Cambridge University Press